THE STAR IDENTIFICATION, POINTING AND TRACKING SYSTEM OF UVSTAR, AN ATTACHED PAYLOAD INSTRUMENT FOR THE SHUTTLE HITCHHIKER–M PLATFORM

Francesco De Carlo, Roberto Stalio, Paolo Trampus
Center for Advanced Research in Space Optics
Area di Ricerca, Padriciano 99, 34012 Trieste, Italy

A. Lyle Broadfoot, Bill R. Sandel
Lunar and Planetary Laboratory, University of Arizona
901 Gould Simpson Building, Tucson AZ 85721

Giovanni Sicuranza
Dipartimento di Elettronica, Elettrotecnica ed Informatica
Università di Trieste, via A. Valerio 10, 34100 Trieste, Italy

ABSTRACT

In this paper we describe an algorithm for star identification and pointing/tracking of a spaceborne electro–optical system and simulation analyses to test the algorithm. The algorithm will be implemented in the guiding system of *UVSTAR*, a spectrographic telescope for observations of astronomical and planetary sources operating in the 500–1250 Å waveband at ≈ 1 Å resolution. The experiment is an attached payload and will fly as a Hitchhiker–M payload on the Shuttle. *UVSTAR* includes capabilities for independent target acquisition and tracking. The spectrograph package has internal gimbals that allow angular movement of $\pm 3°$ from the central position. Rotation about the azimuth axis (parallel to the Shuttle z axis) and elevation axis (parallel to the Shuttle x axis) will actively position the field of view to center the target of interest in the fields of the spectrographs. The algorithm is based on an on–board catalog of stars. To identify star fields, the algorithm compares the positions of stars recorded by the guiding imager to positions computed from the on–board catalog. When the field has been identified, its position within the guiding imager field of view can be used to compute the pointing corrections necessary to point to a target of interest. In tracking mode, the software uses the past history to predict the quasi–periodic attitude control motions of the shuttle and sends pointing commands to cancel the motion and stabilize *UVSTAR* on the target. The guiding imager (guider) will have an 80–mm focal length and f/1.4 optics giving a field of view of $6° \times 4.5°$ using a 385 x 288 pixel intensified CCD. It will be capable of **1)** providing high accuracy (better than 2 arc–sec) attitude determination from coarse ($6° \times 4.5°$) initial knowledge of the pointing direction and **2)** of pointing toward the target. It will also be capable of tracking at the same high accuracy with a processing time of less than a few hundredths of a second.

INTRODUCTION

The determination of the orientation of a satellite or an "attached payload" relative to an inertial reference system, and the correlated functions of acquiring and tracking a target are essential tools for controlling the line of sight of flying electro–optical systems. Among the techniques used for line of sight orientation, automatic identification of stellar fields recorded by one or more dedicated CCD imagers has important applications for delivering space assets to desired locations and/or for pointing spaceborne instruments towards objects of interest. Star field image stabilization with frequent updating of the orientation, using also predictive algorithms, is an additional important function of a modern electro–optical guidance and navigation system. In this paper we describe an algorithm for star identification (Ref. 1, 2) and pointing/tracking of a spaceborne electro–optical system and simulation analyses to test the algorithm. The algorithm will be implemented in the guiding system of *UVSTAR* (Ref. 3). The algorithm is based on an on–board catalog of stars (Ref. 4). To identify star fields, the algorithm compares the positions of stars recorded by the guider to positions computed from the on–board catalog. When the field has been identified, its position within the guider field can be used to compute the pointing corrections necessary to point to a target of interest. In tracking mode, the software uses the past history to predict the quasi–periodic attitude control motions of the shuttle and sends pointing commands to cancel the motion and stabilize *UVSTAR* on the target.

In the next sections we discuss the access to the on–board catalog, the algorithms for automatic star identification and for determining and updating the orientation of the guider, the simulations made and the results obtained in determining the direction of the optic axis of the guider (z axis) under various initial and operating conditions for a system mounted on the Shuttle.

ON – BOARD CATALOG

The on–board catalog used is a subset of the 1991 version of the Smithsonian Astrophysical Observatory (SAO) catalog (1950) (Ref. 4). Only stars with magnitude brighter than 7 are considered. Twenty bytes are reserved to record the parameters of each star: double precision right ascension and declination coordinates and floating point magnitudes. The catalog contains 15935 stars for a total of 318700 bytes.

An access routine to the catalog provides the parameters for the stars contained in a sky zone centered along a given direction. In order to have fast access to any star field, the celestial sphere has been subdivided into 8 "zones" similar to geographic latitude bands. Each zone has been subdivided into "sectors" of equal areas.

Stellar parameters at the beginning and end of each sector are recorded in a table index. The table index is used to quickly select the sector pertaining to the initial direction. Stars of several nearby sectors are also taken into account in order to ensure covering the whole field of view. This accounts for the estimated inaccuracy in the initial estimate of the direction of the guider z axis and for possible guider shifts that may occur during operations.

The simulation of the guider image is generated from the catalogue by projection on the tangent plane. As the polar zones represent a singularity, we treat them independently by means of a reduced catalog. It contains stars north and south of latitudes +45° and -45° respectively. In this catalog the reference celestial coordinates are rotated by 90° around the axis perpendicular to the plane of the celestial pole and vernal equinox axes.

STAR IDENTIFICATION AND ORIENTATION ALGORITHMS

In order to parameterize the rotation of the orthogonal cartesian axes fixed with the guider with respect to an inertial reference frame, we use the rigid body rotation matrix that relates the Shuttle body system to an inertial system. This matrix is expressed in terms of the Euler parameters (quaternions) (Ref. 1, 2), and is initialized to correspond to the estimated direction of the guider z axis. As stated before, the error in this estimate can be as large as a few degrees.

The identification of the stars recorded by the guider is made by comparing these stars with those in the on–board catalog. Before comparison, these last are re–projected on the plane of the guider (a CCD detector) by using the current value of the rotation matrix. The re–projection procedure makes use of the co–linearity formulas (Ref. 2) which, by means of the current value of the rotation matrix, transform stellar celestial coordinates (right ascension and declination) into metric cooordinates (x and y) on the CCD.

The program seeks a one–to–one correspondence between measured inter–angles, i.e. angles under which the guider sees a star pair, and the inter–angles calculated from the catalog stars listed in the appropriate sectors and selected as described above. Two inter–angle tables are constructed: one for the guider stars and one for the catalog stars. An hypothesis of correspondence between the stars listed in the two tables is made. This hypothesis is accepted or rejected by the orientation algorithm. In the case of rejection, another hypothesis is made; and so on.

The algorithm minimizes the distance between guider stars and the hypothezed corresponding ones determined from the catalog. The minimization procedure is made by adjusting the elements of the rotation matrix.

At the end of the procedure we are able

i. to check that the overlap between the catalog and guider stars is achieved (if not, the hypothesis of pair correspondence is rejected; the algorithm then makes another overlap attempt based on a different hypothesis);

ii. to define, starting from the last updating of the rotation matrix, the orientation of the guider rotation relative to the inertial reference system.

An interesting experimental result is that the selection of a large number of stars on the image plane does not raise the algorithm accuracy but, instead, increases calculation time. Therefore a limit of five stars is compared with the catalog stars.

RESULTS OF THE SIMULATIONS

In this section we report our results on the precision in pointing and tracking reached by the algorithm when we add noise to simulate the digitization of star positions. Errors in star position introduced by the optical system are considered negligible and they in fact are with an appropriate choice of the optical system.

In our hypothesis the CCD guider is mounted on a *UVSTAR*–type movable platform on the Shuttle. The requirement is that it must provide autonomous optical fine pointing (± 5 arcsec) within a radius of 3° of the platform nominal view direction, which is near the Shuttle +y axis, i.e. perpendicular to the long axis of the Shuttle and in the plane of the wings. In addition it must provide autonomous tracking for an angular azimuthal movement of $\pm 3°$ around the Shuttle z axis and for an angular elevation movement of $+2°$ to $+8°$ around the Shuttle x axis, measured from the x–y plane.

POINTING

The simulation of the guider image is generated from the catalog on the basis of the following steps:

- access to the catalog in the (nominal) direction of the optical axis of the guider;
- re–projection on a plane tangent to the celestial sphere at the intersection point with the given direction using the "direct" or the "rotated" catalog;
- transformation of star coordinates into pixel coordinates, taking into account the focal length of the guider optics;
- noise addition to the star positions, using a value chosen to simulate the imperfect determination of location on the CCD;

At this point the simulation of the guider image is complete. The algorithm now performs the transformation of star coordinates from pixel into geometrical position on the detector.

The noise in the guider star positions is introduced to simulate the digitization of star coordinates on the CCD. It is expressed as fraction of pixel and represents the interval in which a random variable with uniform distribution is generated. This variable value is algebraically added to the star coordinates. Concerning this last point, one notes that the stars should generally be out of focus and should blur onto several (typically 9) pixels. This allows calculating star positions by centroiding. The adopted perturbations range from ± 0.1 pixel to ± 0.5 pixel, the latter being equivalent to the case in which the stars are focused on a single pixel.

Failure in determining the orientation of the platform occurs when fewer than 3 stars (brighter than 7th magnitude) are in the detector field of view. The probability of this depends on the size of the field of view. One of the fields of view considered corresponds to the design of the guider of the *UVSTAR*. The CCD pixel size considered is 22×22 μm. Table 1 gives the main characteristics

of the electro–optical systems considered. The pixel field of view of about 50 arc–sec represents the theoretical limit of the pointing and tracking method without centroiding; this limit is greatly improved by centroiding.

Figure 1 gives the distribution of number of stars (brighter than $m_V = 7$) for the *UVSTAR* field of view. The diagram has been constructed by simulating 3000 random accesses to different sky zones with the three instruments. The histogram also shows the percentages of times with fewer than three stars, i.e. the percentage of failure in determining the orientation due to insufficient number of stars in the field of view. We detect fewer than three stars only 1.0% of the times. If we adopt two guiding systems with detectors on orthogonal or nearly orthogonal axes, the two percentages become better than 0.01%.

The star identification simulation has been made by random accessing 300 sky zones and running 25 identification cycles per access. At each access the direction of the sky zone was known with a $\pm 3°$ precision. Each cycle has been run by changing in a random way the direction of the optic axis within a circle of 0.2° in order to take into account the maximum perturbation due to the Shuttle movement when it is in "hold mode".

In figure 2 we show the mean error (arc–sec) in the determination of the z–axis direction and the percentage of false identifications ("true failures") as a function of the perturbation. The mean error is better than 4.5 arc–sec and the "true failure" rate is of 2% with a perturbation in 0.2–0.4 pixel range; the error increases almost linearly with the perturbation, i.e. with the added noise. The "true failures" curve displays a strongly increasing slope when the perturbation becomes larger than 0.7, i.e. ± 0.35 pixel. The typical time required to identify the star field is 250 ms using a 25MHz 80386 personal computer with mathematical coprocessor. In figure 3 we show a similar diagram as a function of focal length; it confirms that the best choice for the *UVSTAR* electro–optical system is a 80 mm focal length. In figure 4 we report the mean error (arc–sec) in right ascension and declination as a function of the perturbation.

TRACKING

The goal of tracking is to use the history of the Shuttle attitude, as determined from the guider, to anticipate near–term motions and compute the pointing corrections necessary to cancel them.

In order to generate the simulated CCD images, we have used the parameters of the Shuttle motion recorded during the STS–39 mission. We have considered the temporal variation of the yaw, pitch and roll angles at 1 Hz frequency during 24 hours from MET 475200 s to MET 561600 s; we have extracted and analyzed the data taken when the Shuttle was in inertial hold mode. Given the temporal variation of the yaw, pitch and roll angles in the year 2000 celestial coordinates rest frame, the motion of any vector fixed on the Shuttle body system can be calculated. Figure 5 gives the azimuth (ϕ) and the elevation (θ) variations of the Shuttle vector, in degrees, during the 10 minute interval between MET 542232 to MET 542832 and the absolute value of the differences, in arc seconds, between two successive ($\Delta t = 1$ s) ϕ and θ positions. ϕ and θ are measured in the celestial coordinates reference system.

A recent paper by Neupert *et al.* (1992) on the Orbiter Stability Experiment which has flown on STS–40 shows that the changes in pitch, roll and yaw angles that have been derived from the STS–39 data do not show the real Shuttle motion; these last suffer of jumps with mean amplitude of ≈15 arcsec between two successive (1 Hz) samples which are not recorded by Neupert *et al.* detectors having detection limit of 25 arcsec but sampling frequency larger than 10 Hz. We believe that the STS–39 curves are strongly affected by instrument read–out noise. This effect makes the θ and ϕ curves worse than real curves but, maybe, more interesting for evaluating the performances of the algorithm.

In the tracking mode, once the orientation has been determined with a precision of ±5 arcsec and the sensor is locked on it, the algorithm "follows" the star field by generating "correction curves", $\phi_c(t)$ and $\theta_c(t)$ to the Shuttle motion. Figure 6 gives an example of the calculated $\theta_c(t)$ and the error $\delta\theta(t) = \theta_c(t) - \theta(t)$ using a portion of STS–39 motion record at two perturbation parameters 0.2 and 0.5.

An evaluation of the precision of the method can be obtained by calculating the differences $\delta\theta(t)$, and $\delta\phi(t) = \phi_c(t) - \phi(t)$. Note that interpreting $\delta\phi(t)$, one has to take into account the fact that we are dealing with a dependence on θ. For a particular value of the pointing error δl, measured in the ϕ direction in arc lenght on the sky, $\delta\phi$ is given by $\delta\phi \approx \delta l/\sin\theta$, except near the poles. Therefore $\delta\phi \geq \delta l$, with equality when $\theta = 90°$.

However the division of the celestial sphere into the two parts, polar and equatorial, described above, and their interchanging role, limits the error increment due to the use of angle instead of arc by a safe factor of $\sqrt{2}$. The average values of the errors in ϕ and θ for two different pertubation parameters are reported in Table 2.

The "correction signal" for the motors is derived after the following two steps:

- at a given time t_0 we record the direction of the guider z axis and express it in celestial coordinates;

- at the next step t_1 with the new star field acquisition we calculate the new pointing direction and the new rotation matrix. By means of the co–linearity formulas, we derive the displacement on the CCD plane of the previous z axis direction and express it in microstep pulses to be transmitted to the motor driver.

CONCLUSIONS

The software developed for star field identification and star pointing and tracking demonstrate the capability to reach the high accuracy and precision that are typical characteristics of systems based on stellar sensors. The algorithm has a processing time of less than a few hundredths of a second. This time was in the past the principal limit of this method.

REFERENCES

1. Strikwerda T.E., Junkins J.L., *"Real time spacecraft attitude determination by star pattern recognition: further results"*, 17^{th} Aerospace Science Meeting, New Orleans, 15–17 Jan 1979.

2. Strikwerda T.E., Junkins J.L., *"Star pattern recognition and spacecraft attitude determination"*, Phase II, U.S. Army Corps of Engineers, Engineer Topographic Laboratory, Report for the period Oct. 78–Sep. 79.

3 R. Stalio, B.A. Sandel, A.L. Broadfoot, *"UVSTAR, an Imaging Spectrograph with Telescope for the Shuttle Hitchhiker–M Platform"*, this volume.

4. Documentation for the machine readable version of the S.A.O., version 1984, National Space Data Center, Goddard Space Flight Center

TABLE 1: SIMULATION PARAMETERS OF THE ELECTRO–OPTICAL SYSTEM

Case No.	CCD size (pixel)	Focal length (mm)	Detector FOV	Pixel dimension (arc–sec)
1	385×288	80	6°×4.5°	56

TABLE 2: POINTING PRECISION

Perturbation	$\overline{\delta\theta(t)}$ (arcsec)	$\overline{\delta\phi(t)}$ (arcsec)
±0.2	1.5	1.6
±0.5	8.8	8.5

Fig. 1: Histogram for random accesses to different sky zones at the *UVSTAR* field of view. The vertical axis shows the percentage of the times that n stars brighter than $m_V = 7$ fall in the field of view. The horizontal axis is n.

Fig. 2: The mean error in the determination of the direction of the optical axis and the percentages of failures as a function of the perturbation.

Fig. 3: The ordinate axes give i. the mean value of the error (in arc–sec), ii. the "true failure" rates (in percentage), iii. the percentage of fields with fewer than three stars, iv. the mean time in ms used by the algorithm with the computer system described in the text ($\alpha \approx 50$). The abscissa axis is focal length of the optical system.

Fig. 4: Right ascension and declination errors (in arc–sec) as a function of perturbation.

Fig. 5: Shuttle vector variations during a "hold" period. Top: elevation motion. Bottom: azimuth motion.

Fig. 6: Predictions and prediction errors of the Shuttle motion with two perturbation parameters: 0.2 and 0.5.

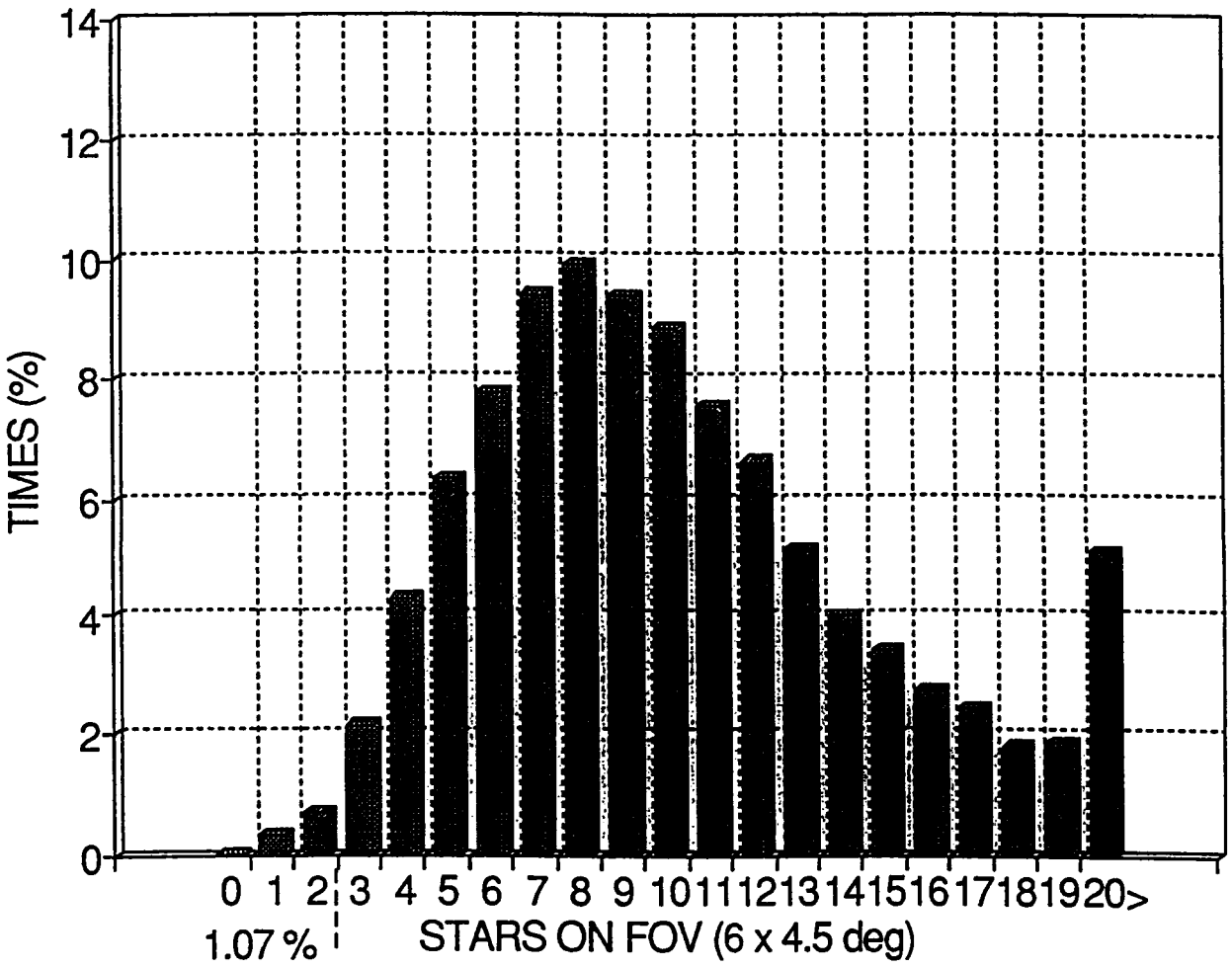

Fig. 1: Histogram for random accesses to different sky zones at the *UVSTAR* field of view. The vertical axis shows the percentage of the times that n stars brighter than $m_V = 7$ fall in the field of view. The horizontal axis is n.

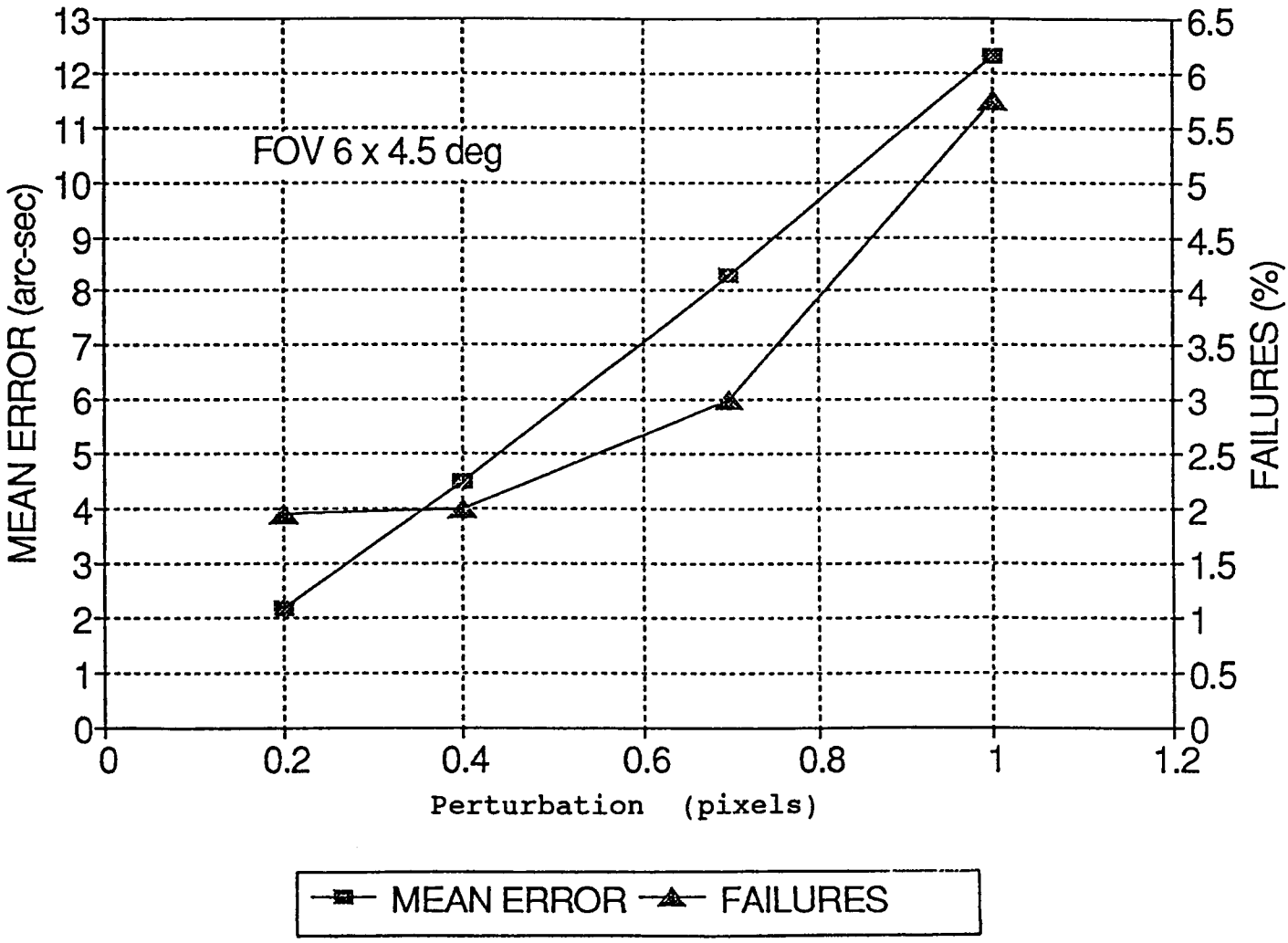

Fig. 2: The mean error in the determination of the direction of the optical axis and the percentages of failures as a function of the perturbation.

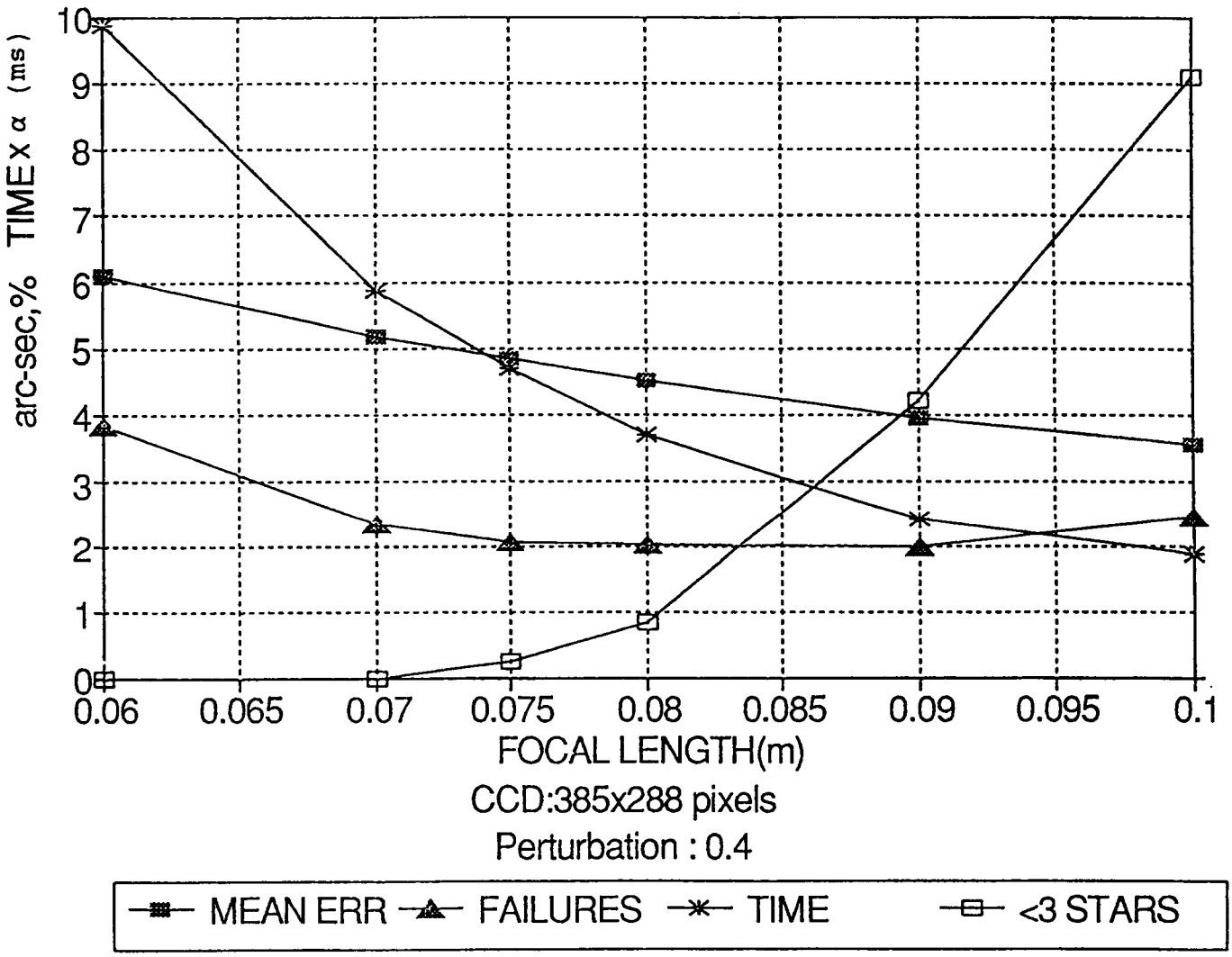

Fig. 3: The ordinate axes give i. the mean value of the error (in arc–sec), ii. the "true failure" rates (in percentage), iii. the percentage of fields with fewer than three stars, iv. the mean time in ms used by the algorithm with the computer system described in the text ($\alpha \approx 50$). The abscissa axis is focal length of the optical system.

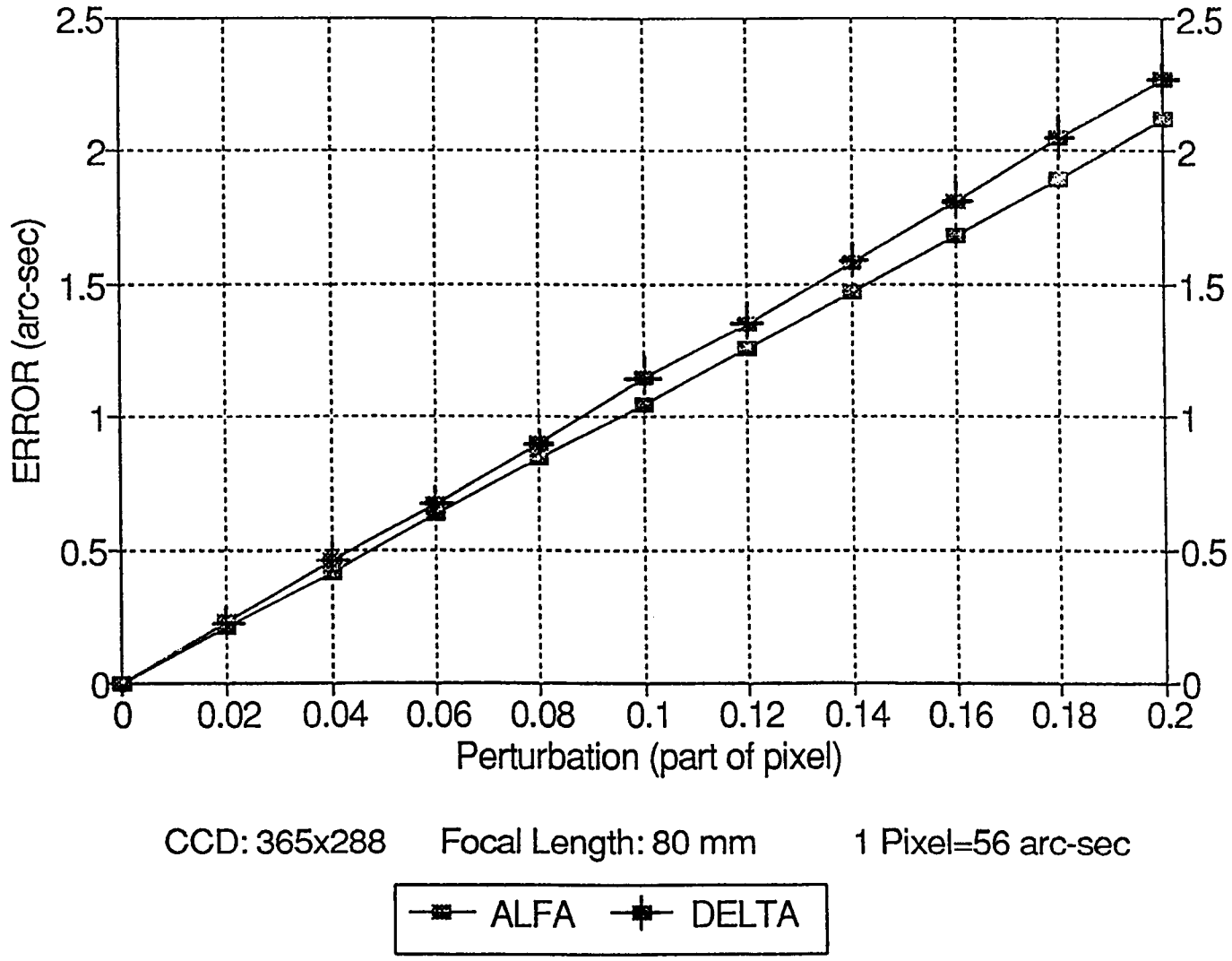

Fig. 4: Right ascension and declination errors (in arc–sec) as a function of perturbation.

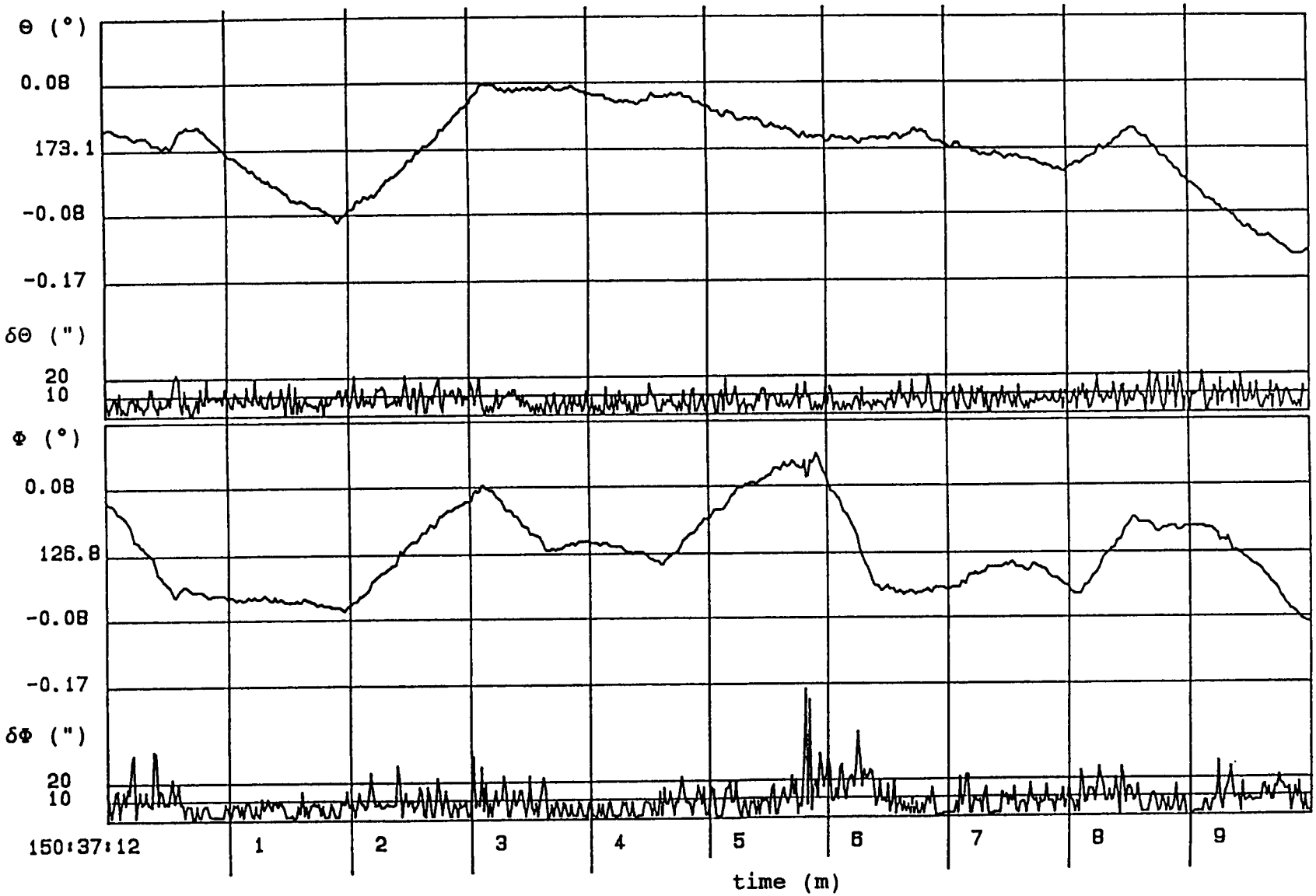

Fig. 5: Shuttle vector variations during a "hold" period. Top: elevation motion. Bottom: azimuth motion.

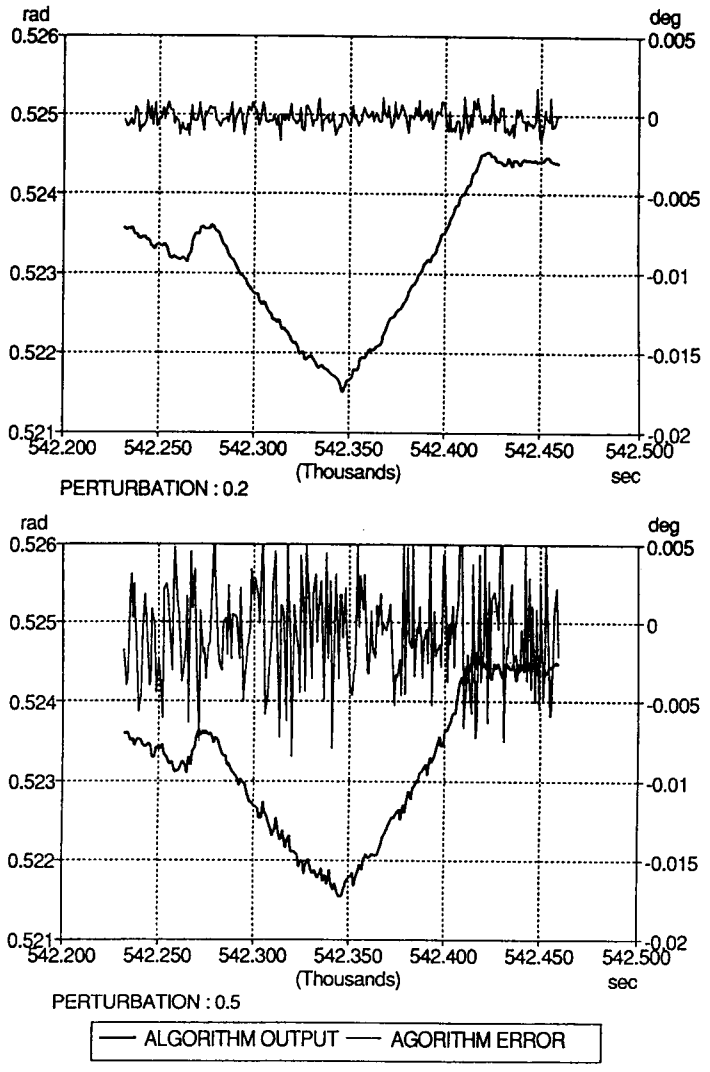

Fig. 6: Predictions and prediction errors of the Shuttle motion with two perturbation parameters: 0.2 and 0.5.